Pharm Res (2015) 32:2259–2265
DOI 10.1007/s11095-014-1615-9

RESEARCH PAPER

Chitosan Nanoparticles for the Linear Release of Model Cationic Peptide

Anna Maria Piras • Stefania Sandreschi • Giuseppantonio Maisetta • Semih Esin • Giovanna Batoni • Federica Chiellini

Received: 21 July 2014 / Accepted: 26 December 2014 / Published online: 6 January 2015

ABSTRACT

Purpose The present study is focused on the development of a model drug delivery system (DDS) based on Chitosan (CS) nanoparticles using Renin substrate I (RSI) as model agent. RSI shares the main chemical-physical features of several biologically active antimicrobial peptides (AMPs). AMPs have a great therapeutic potential that is hampered by their lability in the biological fluids and as such they are perfect candidates for DDS. The development studies of quality DDS loaded with AMPs would require highly sensitive and specific quantification assays. The use of RSI allowed for the fine-tuning and optimization of the formulation parameters to promote the hydrophobic interactions between CS and the cationic peptide, favour the loading of the active ingredient and enhance the release properties of the carrier.

Methods RSI was encapsulated in chitosan NPs by mean of ionic gelation and a chromogenic enzymatic essay was carried out for the release kinetics evaluation.

Results The developed formulations displayed almost 100% of encapsulation efficacy, low burst percentages, and a linear release of the model peptide. A release model was created showing a direct dependence on both the amount of RSI and NPs radius.

Conclusions Although CS has always been formulated with negatively charged active agents (e.g. oligonucleotides or anionic proteins), the use of ionotropic gelation in presence of a small cationic active agent promoted the formation of "core-shell" NPs. The described model, with tuneable linear release rates, appears eligible for further exploitation such as the loading of therapeutically active AMPs.

KEY WORDS antimicrobial peptides · chitosan · drug delivery · linear release · nanoparticles

ABBREVIATIONS

α-CT	α-chymotrypsin
AMC	7-Amino-4-methylcoumarin
AMPs	Antimicrobial peptides
CS	Chitosan
ddH2O	deionised water
DDS	Drug delivery system
DLS	Dynamic light scattering
EE	Encapsulation efficiency
L	Loading content
NPs	Nanoparticles
PEC	Polyelectrolyte complexes
PGA	Poly(γ)-glutamic acid
RSI	Renin Substrate I
SPB	Sodium Phosphate Buffer
STEM	Scanning Transmission Electron Microscopy
TPP	Sodium tripolyphosphate

INTRODUCTION

In recent years, amphipatic cationic peptides have attracted the interest of the scientific community thanks to their high therapeutic potential. Cationic peptides are members of the natural defence of most of living organism and are investigated either as natural derived or as synthetic analogs. Even if they are commonly known as antimicrobial peptides (AMPs),

A. M. Piras · S. Sandreschi · F. Chiellini (✉)
Department of Chemistry and Industrial Chemistry, University of Pisa, UdR INSTM - Pisa, Via Giuseppe Moruzzi 3, 56124 Pisa, Italy
e-mail: federica.chiellini@unipi.it

G. Maisetta · S. Esin · G. Batoni
Department of Translational Research and New Technologies in Medicine and Surgery, University of Pisa, Pisa, Italy

due to the first recognised role of defender against invading pathogens, most of them are also investigated as chemotactic agents, immune modulators and anticancer agents (1). AMPs are relatively small (<10 kDa), with variable length, sequence and structure (2) and exhibit a broad-spectrum activity against a wide range of microorganisms, including multi-resistant isolates of Gram-positive and Gram-negative bacteria species. The hydrophobicity of these peptides is a key parameter in the assessment of selectivity and activity toward pathogens (3–5). Despite an enormous potential for the treatment of infections, the proteolytic degradation of these peptides, their inactivation by anionic albumins and lipoproteins in biological fluids and their potential systemic toxicity are serious limitations to their *in vivo* activity (6). These limitations can be overcome by encapsulation into polymeric nanoparticle (NPs), providing controlled delivery of peptides to eukaryotic and prokaryotic microorganisms growing as planktonic cells as well as biofilms (7). In particular, the development of drug delivery systems (DDS) with linear drug releasing profiles and tunable release rates is generally considered of best importance for the optimization of therapeutic regimens (8).

Chitosan (CS) is a biocompatible and biodegradable polysaccharide obtained by the deacetylation of Chitin; it has been employed in various fields of applications comprising food, biomedicine and agriculture, among others (9). Several studies report on the use of CS for the formulation of micro/nanoparticles as drug delivery systems, either alone or combined into polyelectrolyte complexes (PEC) with alginate or poly(γ)-glutamic acid (PGA) (10,11).

Our previous studies on the use of CS based NPs for the controlled delivery of proteins with antimicrobial activity have shown encouraging results in terms of morphology, full *in vitro* cytocompatibility and a prolonged antimicrobial activity on bacterial strains such as *Staphylococcus epidermidis* (12). Despite the favourable biological properties of CS, its application for the development of NPs by ionotropic gelation is generally associated with negatively charged proteins (or oligonucleotides), in order to promote the electrostatic integrations between the two (13). However, CS possesses hydrophobic ($-CH_3$) and hydrogen bonding favouring moieties (−OH, −NH, and −C=O) and the adjustment of solution pH to neutralize the carried charges is a fundamental aspect exploited for CS thermal gelation (14).

The present study represents the first step for the development of DDS for the controlled release of amphipathic cationic peptides. Renin Substrate I (RSI) (15) was selected as a fluorogenic peptide model for short cationic hydrophobic AMP. The RSI features, such as positive charge at physiological pH (+2), hydrophobicity (62.5% of hydrophobic amino acids) and mass (1301 Da), match with the main characteristics of several AMPs of therapeutic interest comprising those from *Rana temporaria and Rana japonica* (temporin and japonicin-1 families) (16–18), meucin peptides from scorpion (e.g. *Scorpion Mesobuthus eupeus*) (19) and mastoparan peptides from wasp venom (20).

MATERIALS AND METHODS

Materials

CS (weight-average molecular weight Mw 10,8000 g/mol (Mw/Mn 2.4), DD ~92%) (12), sodium tripolyphosphate (TPP), α-chymotrypsin (α-CT) from bovine pancreas and 7-Amino-4-methylcoumarin (AMC) were purchased from Sigma-Aldrich, Milan, Italy. Renin substrate I (Arg-Pro-Phe-His-Leu-Leu-Val-Tyr-AMC) was purchased from Peptide Institute Inc., Osaka, Japan. Acetic acid analytical grade was obtained from Carlo Erba, Milan, Italy. Deionized water (Milli-Q, ddH2O) was used throughout the experiments. Sodium Phosphate Buffer (SPB 10 mM) pH 7.4 was prepared by using dibasic and monobasic sodium phosphate (Sigma-Aldrich, Milan, Italy).

Preparation of Blank or Renin Substrate I-Loaded NPs

NPs were prepared using a simple ionic gelation process (Table I). Briefly, CS was dissolved in 1% (v/v) acetic acid (1 mg/ml, pH 3 or 5) and TPP was dissolved in water (1 mg/ml); for RSI-loaded NPs, 50, 100 or 200 μg of the peptide were added to the CS solution. NPs formed spontaneously upon addition of 2 ml of TPP aqueous solution to 5 ml of the CS/RSI solution under magnetic stirring; the mixture was stirred at room temperature for 2 h.

NPs suspensions were purified by centrifugation in ALC® (Milan, Italy) PK121R centrifuge at 13,000 rpm for 30 min or at 8500 rpm for 60 min, at 4°C.

Characterization of NPs

The size distribution of the developed NPs was measured by mean of dynamic light scattering (DLS) (Coulter LS230 Laser Diffraction Particle Size Analyzer, Beckman Coulter, Nyon, Switzerland). The Zeta-potential of the developed formulations was evaluated using a Beckman-Coulter Delsa™ Nano C, at 25°C in Sodium Phosphate Buffer (SPB 10 mM) pH 7.4. The morphological evaluation of the developed NPs was carried out through Scanning Transmission Electron Microscopy (STEM) by mean of a GEMINI® Multi-Mode STEM (Carl Zeiss Microscopy GmbH, Oberkochen, Germany). Samples were diluted in ethanol (1/200) and directly air dried on formvar-carbon coated copper grids the grid, before the analysis.

Evaluation of RSI Loading Capacity of NPs

The supernatants obtained from NPs purification were submitted to enzymatic digestion by mean of α-chymotrypsin (α-CT). The standard assay mixture contained 80 μl of α-CT solution (0.5 U) in SPB 10 mM, pH 7.4 with 0.1 M $CaCl_2$ and

Table I Main Characteristics of the Prepared NPs: Average Diameter Distribution, Surface Charge, and Loading Capacity

Formulation	pH of CS solution	RSI (μg)	Size (nm ± S.D.)	PdI[a]	Yield (% ± S.D.)	Zeta potential (mV ± S.D.)	L (% ± S.D.)	EE (% ± S.D.)
NPs-A	3	–	140 ± 20	0.001	42.8 ± 0.3	+37.2 ± 1.1	–	–
NPs-B	3	50	107 ± 18	0.002	41.3 ± 0.1	+15.9 ± 0.5	1.0 ± 0.1	56.2 ± 2.3
NPs-C	5	–	124 ± 17	0.001	41.4 ± 0.2	+21.9 ± 0.6	–	–
NPs-D	5	50	195 ± 27	0.002	37.0 ± 0.1	+18.6 ± 0.6	1.8 ± 0.1	96.5 ± 1.4
NPs-E	5	100	310 ± 10	0.046	38.7 ± 0.1	+12.4 ± 0.1	3.6 ± 0.1	97.9 ± 2.1
NPs-F	5	200	390 ± 30	0.133	45.4 ± 0.2	+6.1 ± 1.2	6.0 ± 0.1	97.4 ± 1.5

[a] Polydispersity index of the diameter distribution peak

70 μl of supernatant samples diluted in SPB. The mixture was incubated over night at room temperature and the amount of free AMC was measured at λ_{ex}365 and λ_{em}460 nm using a Victor™ spectrofluorometer (Perkin-Elmer, Monza, Italy). The amount of RSI was calculated from a calibration curve of AMC in SPB (0.012–0.38 μM, R^2 0.9997). The Loading content (L) was defined as the amount of RSI per RSI-loaded NPs dry weight; the Encapsulation efficiency (EE) was defined as the amount of RSI recovered in RSI-loaded NPs compared to the total amount of peptide used in the formulation protocol.

In Vitro Evaluation of RSI Release Kinetics

Purified RSI-loaded NPs were re-dispersed in 1 ml of SPB pH 7.4 (300 μg/ml) and placed into test tubes at 37°C under magnetic stirring. At appropriate intervals, samples were centrifuged at 13,000 rpm 4°C for 30 min, the supernatants were collected and replaced by 1 ml of fresh medium. The amount of RSI released from the NPs was evaluated by α-CT digestion assay as previously described.

The obtained experimental data were submitted to mathematical modeling to formally compare the release kinetics of the three optimized selected formulations (NPs-D, NPs-E and NPs-F).

Peppas equation (21) (Eq. 1) was used to fit experimental data obtained from the release kinetic studies:

$$\frac{M_t}{M_\infty} = kt^n \tag{1}$$

where M_t is the cumulative amount of peptide released at time t, M_∞ is the absolute cumulative amount of peptide released at infinite time (equal to the absolute amount of drug incorporated within the system at time t=0), k is a release rate constant incorporating structural and geometric characteristics of the system and n is the release exponent. To study the release kinetics, data obtained from *in vitro* drug release studies were plotted as cumulative released μg of peptide *versus* time. Knowing M_t, M_∞ and t, the n and k parameters were estimated through a mathematical fit of Peppas equation by mean of IGOR Pro software (WaveMetrics, Portland, USA).

Fick's first law (22) (Eq. 2) was adapted assuming that the difference in the density of the NPs belonging to the three selected formulations is negligible. Moreover, *sink* condition was assumed for the receiver phase, as the peptide concentration in the receiver phase is kept below 1/10 of the peptide concentration in the donor phase (23).

$$\mathcal{J} = \left(\frac{dM}{dt}\right)\frac{1}{S} = -D\left(\frac{dC}{dx}\right) \tag{2}$$

where J is the flux, S is the total surface area crossed by the diffusing species at the rate dM/dt, dC/dx is the concentration gradient and D is the diffusion coefficient. Integrated in time, Fick's first law was rewritten as Eq. 3:

$$M_t = \frac{DCS}{x}t \tag{3}$$

were x is the diffusion layer thickness.

Statistical Analysis

All the characterizations were performed at least on three replicates, unless otherwise specified. The data were statistically analyzed using the Student's t-test. Statistical significance was set at the level of $p<0.05$.

RESULTS AND DISCUSSION

Preparation and Characterization of RSI-Loaded NPs

All the prepared NPs suspensions appeared opalescent and without macroscopically appreciable aggregates. The DLS analysis revealed that the NPs prepared at pH 3 (NPs-A and NPs-B) had mean diameter of 100–140 nm. The change to

pH 5 (NP-C) did not alter significantly the NPs average diameter, but under this formulation condition, the mean diameter of the prepared NPs increased as the amount of RSI loaded in the NPs was heightened (Table I, NPs-D to NPs-F). All the assayed NPs displayed positive Zeta potential values in SPB buffered solutions at pH 7.4.

The STEM morphological analysis evidenced spheroidal particles with nanodimensional size, in line with the diameter range calculated from DLS analysis (Fig. 1). Some particles appeared as elongated structures, but that could be attributed to the formation of aggregates due to sample preparation for STEM analysis. Thanks to the accurate visualization obtained by STEM microscopy and to its sensitivity to density changes of the materials in the analyzed field, STEM microscopy has been used for years for mass-mapping (24). In the present study, the micrographs of RSI-loaded NPs samples (Fig. 1b) displayed nanostructures with a dark dense area covered by a lighter surrounding area, and other smaller particles for which the dense central area is not appreciable. It seems reasonable that the central area corresponded to a packed peptide dense *core* surrounded by a CS rich layer, whereas the smaller round shaped particles were plain CS NPs.

The α-CT digestion of RSI peptide was adjusted for the detection of low amounts of free RSI peptide in SPB solutions, as for the quantification of the peptide released from NPs. The obtained RSI loading capacity and encapsulation efficacy for CS NPs are shown in Table I. Formulation NPs-B (CS at pH 3) proved an E% of 56% and a % of 1%. The EE of RSI was increased to almost the 100% by simply adjusting the CS solution to pH 5 and the L% increased as well, in accordance to the employed drug-polymer ratio.

Evaluation of Drug Release Kinetics

The release kinetic of RSI from RSI-loaded NPs was studied in SPB pH 7.4 for 17 days (Fig. 2). After a first equilibration time (lag time), the system displayed a progressive linear release for all the formulations. During the lag time, the system equilibrated with the release medium; this period was longer for formulations with higher L% values (Table II). In order to formally compare the kinetic release of the three formulations prepared at pH 5 (NPs-D, NPs-E and NPs-F), the RSI release profiles observed after the lag time were submitted to mathematical modeling

A frequently used and easy-to-apply model to describe drug release is Peppas equation (Eq. 1) (21). Peppas' exponent *n* characterizes different release mechanisms from polymeric delivery systems. Table II shows the release exponent values obtained by mean of mathematical fitting of Peppas equation for the selected formulations. Release exponent values were derived for spherical geometries (25,26): n values equal to 0.43 are indicative of a Fickian diffusion; values around 0.85 are related to polymer swelling as the solely release rate controlling mechanism. Release exponents that are in-between these extreme values, as for formulations NPs-D, NPs-E and NPs-F, indicate the so-called "anomalous transport", an overlapping of different types of phenomena, including drug diffusion and polymer swelling.

Table II shows also the equations obtained from the linear interpolation of the release profiles following the lag time. The slope of the obtained line was higher for NPs with higher RSI L% values suggesting that a higher amount of loaded peptide enhanced the release rate, despite the increase in NPs size and the subsequent smaller releasing surface.

Following the observed good linearity of the release profiles and the "*core-shell*" aspect displayed by STEM micrographs, the adaption of Fick's first diffusion law to the prepared drug releasing systems was investigated (22) (Eq. 2).

The slope (m) of the line obtained from the linear fitting of RSI release data was correlated to the parameters of Fick's equation considered constant along the three NPs formulations (D, C and x). For formulation 4 this resulted in Eq. 4:

$$m_{50} = \frac{DC_{50}4\pi {r_{50}}^2 n_{50}}{x} \quad (4)$$

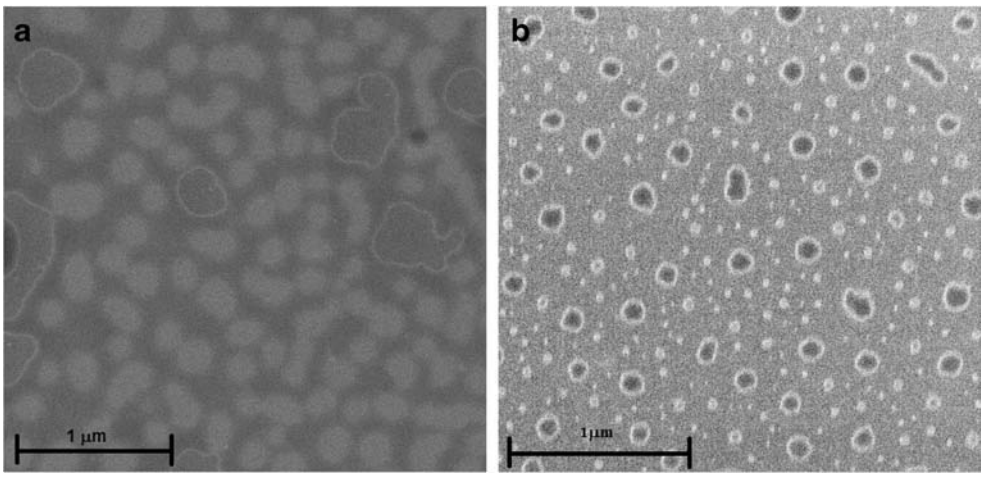

Fig. 1 Morphological characterization of (**a**) Blank nanoparticles (Formulation NPs-A) and (**b**) RSI-loaded nanoparticles (Formulation NPs-B).

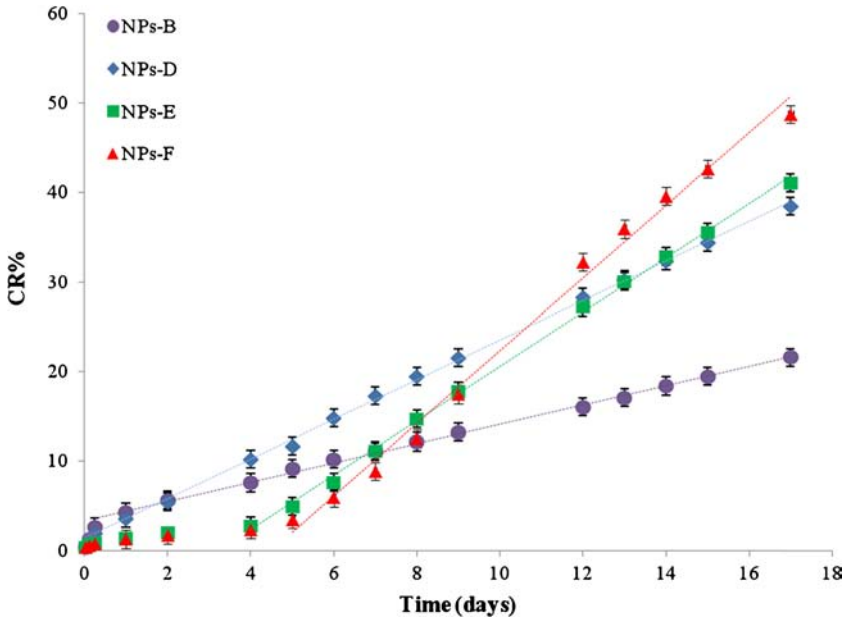

Fig. 2 Release profile of RSI from CS NPs, in SPB pH 7.4, 37°C.

where m_{50} is the slope of the line obtained for formulation NPs-D, C_{50} is the total amount of loaded RSI (mg) for formulation NPs-D, x is the thickness of the NPs membrane and n_{50} is the number of NPs for formulation NPs-D.

Introducing a constant A which includes D, x, 4π and n_{50}, Eq. 4 was rearranged in Eq. 5:

$$m_{50} = AC_{50}{r_{50}}^2 \quad (5)$$

Assuming a similar density, Eq. 4 was written for formulations NPs-E (Eq. 6) and NPs-F (Eq. 7), as well.

$$m_{100} = AC_{100}\frac{{r_{50}}^3}{r_{100}} \quad (6)$$

$$m_{200} = AC_{200}\frac{{r_{50}}^3}{r_{200}} \quad (7)$$

where m_{100} and m_{200} are the slopes of the lines obtained for formulations NPs-E and NPs-F, A is the defined constant and C_{100} and C_{200} are the total amount of loaded RSI (mg) for formulations NPs-E and NPs-F.

Equations 5, 6 and 7 were used to calculate the constant value A for formulations NPs-D, NPs-E and NPs-F, respectively. The obtained A values are shown in Table II: the differences between the constants calculated from the three formulations were not statistically significant ($p>0.05$, Student's T test), proving that the variations in the release rates were only dependent on the amount of loaded peptide and NPs radius. Moreover, the accordance between the observed linear slopes and the slopes values determined from Eqs. 5, 6 and 7 reached almost 100% for all the formulations.

DISCUSSION

CS NPs were easily prepared by mean of ionic gelation between cationic chitosan and anionic TPP. Ionic gelation was performed at two different pH of the CS solution, pH 3 and pH 5. CS is a weak base polysaccharide, having an average amino group density of 0.837 per disaccharide unit, insoluble at neutral and alkaline pH values. In an acidic medium, the amine groups will be positively charged, conferring to the polysaccharide a high charge density (27). Though CS NPs are usually formed from CS solution at pH 3, in this study the

Table II Mathematical Modeling of RSI Release Kinetics. T_L is the Lag Time; CR% is the Cumulative Release in Percentage at the Lag Time (T_L) and at 17 days (T_{17}); % Acc. is the Correlation Between Model Theoretical and Experimental Data for Fickian Diffusion Model. The Values are Expressed ± Standard Deviation

Formulation	T_L (h)	CR % at T_L	CR % at T_{17}	Peppas			Linear regression (R^2)	Fickian diffusion	
				k	*n*	X^2		A	% Acc.
NPs-B	6	2.6	21.6	0.0092 ± 0.0002	0.7377 ± 0.034	0.87	*y* = 0,0456x + 3,207 (0,9979)	–	–
NPs-D	6	1.9	38.5	0.0100 ± 0.0002	0.7116 ± 0.017	0.66	*y* = 0,0916x + 1,444 (0,9994)	0.00020 ± 0.00006	99.36
NPs-E	96	2.7	41.1	0.0023 ± 0.0003	0.7897 ± 0.012	0.91	*y* = 0,1185x − 8,142 (0,9951)	0.00021 ± 0.00009	98.99
NPs-F	120	3.6	48.7	0.0055 ± 0.0002	0.8369 ± 0.013	1.23	*y* = 0,1609x − 16,561 (0,9933)	0.00018 ± 0.00008	100.00

pH of the polymer solution was raised to 5 (avoiding CS precipitation), in order to reduce the charge repulsion between cationic chitosan and cationic RSI. Thus, promoting the peptide encapsulation in NPs through the hydrophobic interaction between CS backbone and RSI. The pH change from 3 to 5 of the formulation conditions was reflected in a variation of the Z potential values (formulation NPs-A and NPs-C), confirming a different arrangement of the CS chains during the ionic gelation process (28). The loading of RSI in the NPs brought a decrease of the positive Zeta potential values, with statistically significant differences ($p < 0.05$, Student's t test) between the formulations NPs-D, NPs-E and NPs-F. These Z-potential changes may be attributed to conformational and charges rearrangements caused by the loading of the peptide in the NPs.

Being a cationic peptide, RSI is favourable to crosslink in presence of TPP (polyanion). Preliminary evaluation of RSI capability of crosslinking in presence of TPP was performed in 1% (v/v) acetic acid at both pH 3 and 5. After 40 min, the RSI TPP mixtures displayed aggregates with diameter in the range of 6–9 μm, as estimated by Delsa™ Nano C photocorrelation analysis. For the preparation of the NPs, RSI was placed in presence of CS and thanks to its smaller size, it is reasonable that it was assembling faster to form the dense peptide rich core observed in the STEM micrographs, covered by the outer CS layer. Moreover, the small empty NPs observed in Fig. 1b can then be attributed to residual plain CS crosslinked with TPP.

In order to evaluate RSI loading and release from the prepared NPs, an enzymatic assay for peptide digestion was developed and optimized. RSI is usually employed in fluorometric assays to detect Proteinase A from yeast or as Renin substrate; α-CT is a well-known serine protease that catalyzes the hydrolysis of peptide bonds on the C-terminal side of tyrosine residues. These substrate and enzyme, commonly employed separately as reported by the literature (29,30), were here employed together for a rapid and inexpensive fluorometric assay. The sensitivity of the assay allowed for the easy detection of the unloaded and of the released peptide down to 12 nM concentrations.

CS based NPs are generally describible as nanogels, in which the loaded drug is dispersed in the reticulated chitosan matrix (31). In the present work, the cationic peptide took part to the ionotropic gelation and the promoted interaction between CS and RSI (obtained by pH modulation) determined the packing of the peptide at the centre of the particle, with E% of about 100%. The stability of CS based NPs placed in SPB at 37°C was assessed in a previous work. After 5 days a small increase of the nanoparticles mean diameter was observed and associated to the swelling and water adsorption of the system. Furthermore, CS molecular weight was also monitored and no hydrolysis or degradation occurred (12). Even though the observed diameter increase supports the general assumption that the releasing mechanism is guided by swelling phenomena and drug diffusion through the hydrated matrix, the present CS NPs appeared more as pseudo "reservoir" devices, with the peptide forming an inner *core* surrounded by a peptide poor layer (22). The adaption of the Fickian drug diffusion model gave the better results in terms of correlation between theoretical modeling and experimental data. Furthermore, the developed mathematical model can be used for a release rate anticipation employing NPs radius and peptide loading as the only variable parameters. Additional investigations to assess if the drug release rate is affected by the dissociation of the complexes between TPP and the cationic peptide, will be carried out.

CONCLUSIONS

The proposed CS NPs model possesses ideal characteristics for the loading of cationic hydrophobic peptides of biomedical/medical relevance, allowing for almost 100% of peptide encapsulation efficacy. Thereby, the waste of expensive and precious materials such as peptides is highly limited.

The developed model will be exploited for the loading of selected AMPs with antibacterial features. The linear kinetic of AMPs release by CS NPs may be useful for the therapy of chronic or biofilm-realated infections. In these cases, the prolonged release of AMPs may also reduce the incidence of infection relapses.

ACKNOWLEDGMENTS AND DISCLOSURES

The authors would like to acknowledge the contribution given by Dr. Giovanni Baldi, Dr. Filippo Mazzantini and Dr. Costanza Ravagli in recording STEM images of NPs.

REFERENCES

1. Conlon JM, Mechkarska M, Lukic ML, Flatt PR. Potential therapeutic applications of multifunctional host-defense peptides from frog skin as anti-cancer, anti-viral, immunomodulatory, and anti-diabetic agents. Peptides. 2014;57:64–77.
2. Hancock R. Cationic antimicrobial peptides: towards clinical applications. Exp Opin Invest Drugs. 2000;9(8):1723–9.
3. Henriksen J, Etzerodt T, Gjetting T, Andresen T. Side chain hydrophobicity modulates therapeutic activity and membrane selectivity of antimicrobial peptide mastoparan-X. PLoS ONE. 2014;9(3):e91007.
4. Jiang Z, Vasil AI, Gera L, Vasil ML, Hodges RS. Rational design of alpha-helical antimicrobial peptides to target Gram-negative pathogens, Acinetobacter baumannii and Pseudomonas aeruginosa: utilization of charge, 'specificity determinants', total hydrophobicity, hydrophobe type and location as design parameters to improve the therapeutic ratio. Chem Biol Drug Des. 2011;77(4):225–40.
5. Sato H, Feix JB. Peptide-membrane interactions and mechanisms of membrane destruction by amphipathic alpha-helical antimicrobial peptides. Biochim Biophys Acta. 2006;1758(9):1245–56.

6. Yeung AY, Gellatly S, Hancock RW. Multifunctional cationic host defence peptides and their clinical applications. Cell Mol Life Sci. 2011;68(13):2161–76.
7. Brandelli A. Nanostructures as promising tools for delivery of antimicrobial peptides. Mini Rev Med Chem. 2012;12:731–41.
8. Xiong MH, Bao Y, Yang XZ, Zhu YH, Wang J. Delivery of antibiotics with polymeric particles. Adv Drug Deliv Rev. 2014.
9. Denkbas EBOR. Perspectives on: chitosan drug delivery systems based on their geometries. J Bioact Compat Polym. 2006;21:351–68.
10. Su F-Y, Lin K-J, Sonaje K, Wey S-P, Yen T-C, Ho Y-C, *et al.* Protease inhibition and absorption enhancement by functional nanoparticles for effective oral insulin delivery. Biomaterials. 2012;33(9):2801–11.
11. Yang S-J, Lin F-H, Tsai H-M, Lin C-F, Chin H-C, Wong J-M, *et al.* Alginate-folic acid-modified chitosan nanoparticles for photodynamic detection of intestinal neoplasms. Biomaterials. 2011;32(8):2174–82.
12. Piras AM, Maisetta G, Sandreschi S, Esin S, Gazzarri M, Batoni G, *et al.* Preparation, physical-chemical and biological characterization of chitosan nanoparticles loaded with lysozyme. Int J Biol Macromol. 2014;67:124–31.
13. Gan Q, Wang T. Chitosan nanoparticle as protein delivery carrier—systematic examination of fabrication conditions for efficient loading and release. Colloids Surf B: Biointerfaces. 2007;59:24–34.
14. Cho J, Heuzey M, Bégin A, Carreau PJ. Physical gelation of chitosan in the presence of β-glycerophosphate: the effect of temperature. Biomacromolecules. 2005;6:3267–75.
15. Murakami K, Ohsawa T, Hirose S, Takada K, Sakakibara S. New fluorogenic substrates for renin. Anal Biochem. 1981;110(1):232–9.
16. Eckert R. Road to clinical efficacy: challenges and novel strategies for antimicrobial peptide development. Rev Future Microbiol. 2011;6(6):635–51.
17. Isaacson T, Soto A, Iwamuro S, Knoop FC, Conlon JM. Antimicrobial peptides with atypical structural features from the skin of the Japanese brown frog Rana japonica. Peptides. 2002;23(3):419–25.
18. Mangoni ML, Saugar JM, Dellisanti M, Barra D, Simmaco M, Rivas L. Temporins, small antimicrobial peptides with leishmanicidal activity. J Biol Chem. 2005;280(2):984–90.
19. Gao B, Sherman P, Luo L, Bowie J, Zhu S. Structural and functional characterization of two genetically related meucin peptides highlights evolutionary divergence and convergence in antimicrobial peptides. FASEB J. 2009;23(4):1230–45.
20. Sample CJ, Hudak KE, Barefoot BE, Koci MD, Wanyonyi MS, Abraham S, *et al.* A mastoparan-derived peptide has broad-spectrum antiviral activity against enveloped viruses. Peptides. 2013;48:96–105.
21. Peppas NA. Analysis of Fickian and non-Fickian drug release from polymers. Pharm Acta Helv. 1985;60(4):110–1.
22. Baker R, Lonsdale H. Controlled release of biologically active agents. New York: Plenum Press; 1974. p. 15–72.
23. Gibaldi M, Feldman S. Establishment of sink conditions in dissolution rate determinations. Theoretical considerations and application to nondisintegrating dosage forms. J Pharm Sci. 1967;56(10):1238–42.
24. Thomas D, Schultz P, Steven AC, Wall JS. Mass analysis of biological macromolecular complexes by STEM. Biol Cell. 1994;80(2–3):181–92.
25. Ritger PL, Peppas NA. A simple equation for description of solute release II. Fickian and anomalous release from swellable devices. J Control Release. 1987;5(1):37–42.
26. Ritger PL, Peppas NA. A simple equation for description of solute release I. Fickian and non-fickian release from non-swellable devices in the form of slabs, spheres, cylinders or discs. J Control Release. 1987;5(1):23–36.
27. Ko JA, Park HJ, Hwang SJ, Park JB, Lee JS. Preparation and characterization of chitosan microparticles intended for controlled drug delivery. Int J Pharm. 2002;249(1–2):165–74.
28. Gan Q, Wang T, Cochrane C, McCarron P. Modulation of surface charge, particle size and morphological properties of chitosan-TPP nanoparticles intended for gene delivery. Colloids Surf B: Biointerfaces. 2005;44(2–3):65–73.
29. Yokosawa H, Ito H, Murata S, Ishii S. Purification and fluorometric assay of proteinase A from yeast. Anal Biochem. 1983;134(1):210–5.
30. Burrell M, Sweeney P, Walker J. Proteolytic enzymes for peptide production. In: Press H, editor. Enzymes of molecular biology. 1993. p. 277.
31. Yoksan R, Chirachanchai S. Amphiphilic chitosan nanosphere: studies on formation, toxicity, and guest molecule incorporation. Bioorg Med Chem. 2008;16(5):2687–96.